Journal of Engineering Mathematics **35:** 109–117, 1999.

Generation of ripple-size internal waves on a fluidized seafloor

(The Ephemeral Ripples)

MOSTAFA A. FODA
Environmental Water Resources, Department of Civil and Environmental Engineering, University of California, Berkeley, CA 94720, U.S.A.

Received 8 August 1997; accepted in revised form 1 July 1998

Abstract. Ripples produced on a fluidized seafloor have been observed in the field as well as in the laboratory. Because of their dynamic properties, they are sometimes referred to as *transitional* or *ephemeral* ripples, as they have been observed to go through cycles of forming and disappearing on the time scale of an individual wave period. The ripples also appear to go through a complex evolutionary sequence, occasionally leading to the spectacular event of sediment *bursting* from the seafloor. During bursting, loads of fluidized sediment will be ejected upward into the water column – in the form of intense sand plumes. Reproducing these ripples in the laboratory revealed that these ripples are actually a standing subharmonic internal wave on the water-sediment interface, produced by the water wave propagating above through an instability mechansim. In this paper an inviscid theory for the initial excitation of these dynamic ripples on a fluidized seafloor is presented.

Key words: ripples, seafloor, ocean mechanics, sediments, water waves

1. Introduction

In the coastal zone, loading from progressive wind waves can cause fluidization of bottom sediment within a thin surface-layer in the seabed. Fluidization is defined as the process by which a soil mass loses its shear rigidity and behaves much like a fluid. The thickness of the fluidized layer will of course depend on the severity of the wave loading, and the exact mechanism of fluidization appears to be quite complex and not yet well understood [1]. However, once fluidization starts to occur, a variety of processes may begin to take place, involving exchanges of significant amount of mass across the seafloor as well as the spreading and transport of loads of sediment laterally over the seafloor, and possibly some progressive and extensive soil failure events in the seabed. Recently, Foda and Huang [2] reported on a laboratory flume observation of the post-fluidization behavior of a bed-water interface under a progressive shallow-water wave. In some runs, they observed that the loading from the surface water wave on the fluidized sediment bed has excited a nearly standing subharmonic internal wave on the interface. The excited internal wave has a ripple-size wavelength, which is an order-of-magnitude smaller than the wavelength of the generating surface wave.

On the other hand, it is common knowledge that shallow-water waves propagating over a bed of sand often distort the bed into a pattern of bed forms or ripples. Bed ripples have significant influences on near-bed currents, marine sediment transport and wave height attenuation in the coastal zone. This has motivated extensive research on wave-induced rippling and associated effects in the coastal-engineering literature (see, *e.g.* [3] for a review). Furthermore, *relic* ripples in sedimentary records provide important clues to geologists on past wave climates in a region, and hence may help infer, among other things, the geological sealevel fluctuations there.

Most of the laboratory studies on wave-induced ripples were concerned with the so-called *permanent* ripples, *e.g.* vortex or rolling-grain ripples [3] under relatively small-amplitude waves. These waves were too small to generate a fluidized *sheet-flow* on the bed surface. Most of the permanent ripples are two-dimensional, *i.e.* a ripple crest is parallel to the wave crest, with the ripples being regularly spaced and nearly sinusoidal in shape. Recently, Conley and Inman [4] conducted a field study to observe the seafloor behavior under stronger wave loading, characterized by a large enough Shields number to force sheet flows on the seafloor. Instead of the permanent ripples, they sometimes observed what they termed transitional, or *ephemeral ripples.* These ripples keep forming and disappearing in the time scale of individual waves. Inman [5] who first reported on these ephemeral ripples observed them near the surf zone, where sediment motion during their presence was described as a 'dense layer of suspended particles'. Conley and Inman [4] further examined the structures of these ripples, as they often begin by having a clear three-dimensional pattern, which sometimes further evolves and reorganizes into the two-dimensional ripples. This ultimately results in an occasional but explosive *bursting*, or ejection of some of the sediment slurry up into the water column, in the form of isolated intense sand plumes. One curious observation of Conley and Inman, however, was that these ripples and the associated occasional bursting appeared *only* under a wave crest, but *not* under the trough.

The experiment by Foda and Huang [2] was the first successful attempt to recreate these ephemeral ripples in the laboratory.

There are many similarities between these laboratory ripples and those observed by Conley and Inman [4] in the field. They have similar sizes. They also appeared under one half of the wave cycle (crest), and disappeared in the other half (trough) during their experiments. The observation that these ripples are in fact a standing subharmonic internal waves provides a simple explanation of this behavior, as illustrated in the sketches of Figure 1. The figure shows a sequence of the wave-seafloor profiles at intervals of $0{\cdot}5T$, with T being the water wave's period. The sketches show a flat seafloor alternating with a rippled one, a simple property of a standing wave. This obviously gives the impression that the ripples are forming and disappearing within a single wave cycle. Actual photographs of this sequence, taken during the laboratory experiments are reproduced in [6].

In this paper, we present an instability theory to explain the initial generation of these ephemeral ripples on a fluidized seafloor. A more general instability mechanism for the generation of internal waves by a *single* surface wave has been reported already in recent papers by Hill and Foda [6, 7] and Foda and Hill [8]. The emphasis in these papers, however, was on typical oceanographic stratification induced by salinity-temperature variations in the ocean. Here, we present the theory within the context of the much stronger density stratification induced by sediment fluidization processes in shallow coastal waters.

2. Formulation of the problem

Surface waves have long been identified as one of the possible energy sources for the generation of internal waves in the marine environment. However, direct resonance has been generally ruled out as an important mechanism for the transfer of energy from surface to internal modes. This is because the Brunt-Vaisala wave-period in a stratified sea, which represents the lower bound for internal-wave periods, is typically of the order of a few minutes

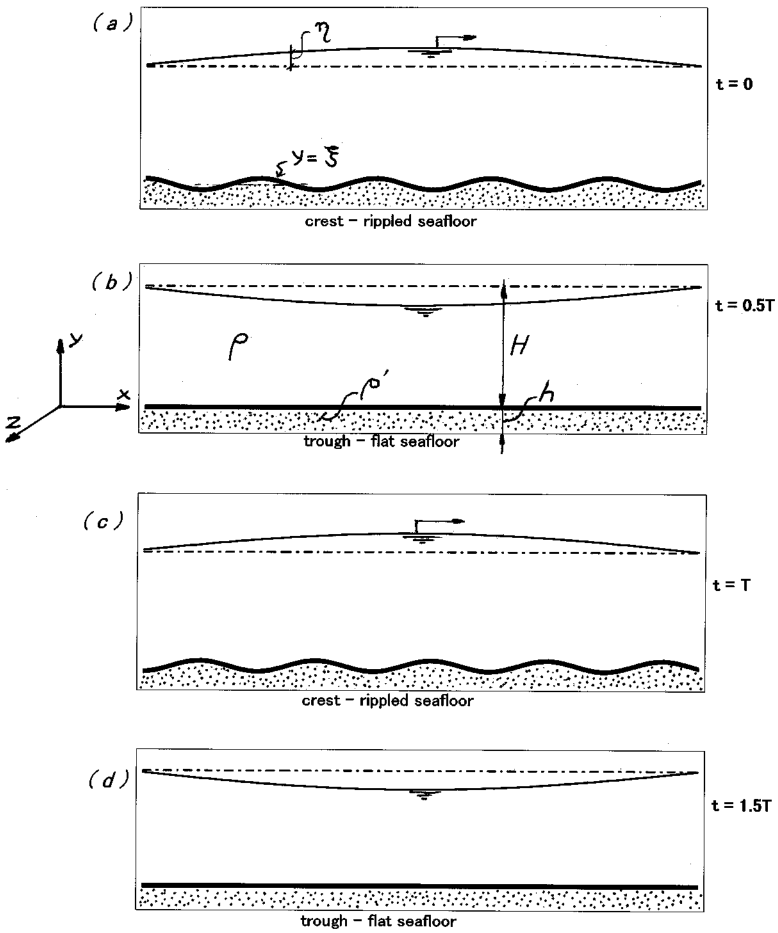

Figure 1. Sketches of the water wave – seafloor profiles at $0{\cdot}5T$ intervals, T being the water-wave period. The fluidized seafloor is fluctuating as a standing sub-harmonic wave. Note that the ripples in (a) are out of phase with the ripples in (c).

or longer. This is much longer than periods of the most energetic surface wind waves; around ten seconds or so.

One important exception to the above is in a shallow coastal environment, where water stratification may be greatly enhanced by a significant load of bottom sediment in a state of suspension or fluidization. The sediment suspension-load may result in a stronger density gradient across the water column, and hence a large reduction in the Brunt-Vaisala period – approaching that of surface gravity waves. Here, we assume such strong stratification and propose a wave-triad resonance between a single progressive surface wave and a pair of internal wave perturbations. The internal waves would form a nearly standing, subharmonic wave on the sediment-water interface.

As shown in Figure 1 the origin of a three dimensional Cartesian coordinate system is placed on the undisturbed interface between the seabed and a water layer of depth H and density ρ. Below the origin, we assume that a very thin surface layer of the seabed, of thickness $h \ll H$, has been fluidized, with the resulting slurry having a density of $\rho' > \rho$, or $\gamma = \rho/\rho' < 1$. For simplicity, we assume here that both water and slurry are inviscid, and focus on the effect of density stratification on the ensuing interaction. Further, we assume that below the fluidized sediment layer, the seabed is rigid.

We let a surface gravity wave of amplitude A, frequency ω and wavenumber k propagate in the positive x direction, and introduce a pair of generally oblique internal wave perturbations on the fluidized seafloor $z = 0$, as shown in Figure 1. The objective then is to investigate whether the oblique internal-wave perturbations can extract energy from the surface wave, and as a result grow in time. Initially, the perturbation internal waves have amplitudes a_1 and $a_2 \ll A$, wavenumber vectors λ_1 and λ_2, and frequencies σ_1 and σ_2. For resonant interaction to occur, the following conditions are imposed on the triad's wavenumber components and frequencies where

$$\lambda_{2x} - \lambda_{1x} = k, \qquad \lambda_{2z} = \lambda_{1z}, \qquad \sigma_1 + \sigma_1 = \omega,$$

where $\lambda_i = \lambda_{ix}, \lambda_{iz}$; $(i = 1, 2)$, are the components of the internal waves' pair of wavenumber-vectors in the x and z directions, respectively. Without any loss of generality, we assume here that λ_{1z}, λ_{2z}, σ_1, σ_2, and ω are all real *and positive*. The x-components of the internal wavenumber vectors λ_{1x} and λ_{2x} are assumed real but allowed to be either positive or negative, depending on whether the internal wave is propagating in the positive or negative x-directions (either direction is possible, of course).

Expressing the flow-field in the two-layer inviscid system in terms of a velocity potential Φ, we see that Φ satisfies Laplace's Equation throughout the depth of the fluid.

$$\nabla^2\Phi = 0, \quad -h \leqslant y \leqslant H + \eta, \tag{1}$$

where η is the displacement of the water surface from its static elevation $y = H$. At the free surface, there are the usual kinematic and dynamic conditions

$$\frac{\mathrm{D}\eta}{\mathrm{D}t} = \Phi_y, \quad y = H + \eta, \tag{2}$$

$$\Phi_t + g\eta + \tfrac{1}{2}\nabla\Phi \, . \, \nabla\Phi = 0, \quad y = H + \eta. \tag{3}$$

The interface between the water and the slurry will be displaced by ξ from its static elevation $y = 0$, due to the presence of the waves. Similar conditions of continuity of normal velocities and traction stresses are imposed at the disturbed interface

$$\frac{\mathrm{D}\xi}{\mathrm{D}t} = \Phi_y^+ = \Phi_y^-, \quad y = \xi, \tag{4}$$

$$\rho(\Phi_t + g\xi + \tfrac{1}{2}\nabla\Phi \, . \, \nabla\Phi)^+ = \rho'(\Phi_t + g\xi + \tfrac{1}{2}\nabla\Phi \, . \, \nabla\Phi)^-, \quad y = \xi. \tag{5}$$

And finally, at the bottom of the fluidized slurry, we have the no flux condition

$$\Phi_y = 0, \quad y = -h. \tag{6}$$

By construction, we have three free wave harmonics in the velocity potential Φ, *i.e.* we assume the following expansion for Φ:

$$\Phi = \varepsilon\phi \, \mathrm{e}^{i(kx-\omega t)} + \varepsilon^2\{\psi \, \mathrm{e}^{i(\lambda_{1x}x-\lambda_{1x}z+\sigma_1 t)} + \chi \, \mathrm{e}^{i(\lambda_{2x}x-\lambda_{2x}z-\sigma_2 t)}\} + \Phi_{n.l.} + \text{c.c.} \, . \tag{7}$$

The first three terms of the above expansion represent the three free harmonics; first term is the surface wave, and the following two terms are for the internal waves. $\Phi_{n.l.}$ represents the forced component of the velocity potential due to nonlinear interaction among these free three harmonics, and *c.c.* denotes complex conjugate. The expansion parameter ε is assumed to be proportional to the steepness of the surface wave, *i.e.* $\varepsilon \sim kA \ll 1$, and we restrict the analysis here to the case of small internal waves so the internal wave perturbations appear at $O(\varepsilon^2)$ and not at $O(\varepsilon)$.

3. Quadratic interaction and the growth of the seafloor waves

The solution procedure follows a standard perturbation analysis for a weakly nonlinear wave-field system (see, *e.g.* [9]). The procedure involves solving the above BVP problem in an ordered sequence, by separating terms in the governing equations and the boundary conditions according to their order in ε and their phase. It then follows that all the terms of the same order and the same harmonic would have to be balanced separately from all the other terms. Then, starting at the leading $O(\varepsilon)$ order, we solve for each harmonic, separately, and proceed successively into higher orders.

At the leading order, we have three approximate linear solutions for the interacting harmonics:

Surface wave

$$\phi = \frac{-igA}{\omega \cosh(kH)} \cosh(ky), \quad y > 0, \tag{8}$$

$$\phi = \frac{-i\gamma gA}{\omega \cosh(kH)} \cosh(ky), \quad y < 0, \tag{9}$$

$$\omega^2 = gk \tanh(kH); \tag{10}$$

Short Internal wave 1

$$\psi = \frac{-i\sigma_1 a_1}{\lambda_1} \mathrm{e}^{-\lambda_1 y}, \quad y > 0, \tag{11}$$

$$\psi = \frac{i\sigma_1 a_1}{\lambda_1 \sinh(\lambda_1 h)} \cosh[\lambda_1 (h + y)], \quad y < 0, \tag{12}$$

$$\sigma_1^2 = \frac{g(1-\gamma)\lambda_1}{\gamma + \coth(\lambda_1 h)}; \tag{13}$$

Short Internal wave 2

$$\chi = \frac{i\sigma_2 a_2}{\lambda_2} \mathrm{e}^{-\lambda_2 y}, \quad y > 0, \tag{14}$$

$$\chi = \frac{-i\sigma_2 a_2}{\lambda_2 \sinh(\lambda_2 h)} \cosh[\lambda_2 (h + y)], \quad y < 0, \tag{15}$$

$$\sigma_2^2 = \frac{g(1-\gamma)\lambda_2}{\gamma + \coth(\lambda_2 h)}. \tag{16}$$

Because we are assuming that the internal waves are short relative to the water depth H, they are not feeling the presence of the free surface, as implied in the above solutions.

At the second order, $O(\varepsilon^2)$, quadratic interactions between the above linear harmonics give rise to secular term forcing on the right-hand sides of the nonlinear boundary conditions (4) and (5). Invoking solvability, through the use of Green's theorem (see, *e.g.*, [6] for details), we obtain the desired evolution equations for the internal wave amplitudes. For simplicity, we present the results here for the case of a shallow-water depth for the surface wave, and a shallow lower-layer depth for the internal waves, *i.e.*

$$kH, \lambda_1 h, \lambda_2 h \ll 1. \tag{17}$$

Under these simplifying assumptions, the amplitude equations – via solvability – may be straightforwardly shown to be given by

$$\frac{\mathrm{d}^2 a_i}{\mathrm{d}t^2} - \alpha^2 a_i = 0, \quad i = 1, 2, \tag{18}$$

$$\alpha = \tfrac{1}{2}|A|\left\{-\frac{g}{H}\left(1 - 2\gamma\frac{\sigma_2}{\sigma_1} + \frac{k}{\lambda_{1x}}\right)\left(1 - 2\gamma\frac{\sigma_1}{\sigma_2} - \frac{k}{\lambda_{2x}}\right)\lambda_{1x}\lambda_{2x}\right\}^{1/2}. \tag{19}$$

If α is purely imaginary, then the amplitudes a_1 and a_2 will not grow with time, or equivalently, the surface wave is being stable to these internal wave perturbations. Growth will occur only when α is real. Because of the compactness of the result in (18), the property of the instability mechanism and its dependence on the various physical parameters can be readily and easily assessed here.

4. Discussion and conclusion

Examining the expression for the *growth rate* α as given in (19) we see that there are – in general – two obvious possibilities for making α real. One is when at least one of the ratios k/λ_{ix} is large enough so that the two brackets under the square-root in (19) will be of different signs. The second is when λ_{1x} and λ_{2x} are themselves of different signs. Physically, the first possibility corresponds to at least one of the internal waves being almost perpendicular to the surface wave. The second possibility corresponds to the two internal waves having x-propagation in the positive x-direction, following the surface wave. These and other, less obvious possibilities will now be investigated in some detail.

First, let us consider the 2-D case of all three free waves propagating in the x plane, *i.e.* no obliqueness between the surface and internal modes. In this case, $\lambda_{1z} = \lambda_{2z} = 0$. From the dispersion relations, assuming comparable frequencies in order to satisfy resonance, we see that the wavenumbers ratios are of the following order of magnitude

$$(k/\lambda_{ix})^2 \sim (1-\gamma)h/H \ll 1, \quad i = 1, 2. \tag{20}$$

Returning to (19), it is clear then – because of the smallness of the ratios k/λ_{ix} – that α will always be purely imaginary in this case. The two brackets under the square-root are always of the same sign in the 2-D case! This means that the 2-D case is always stable. This reproduces the finding of [6].

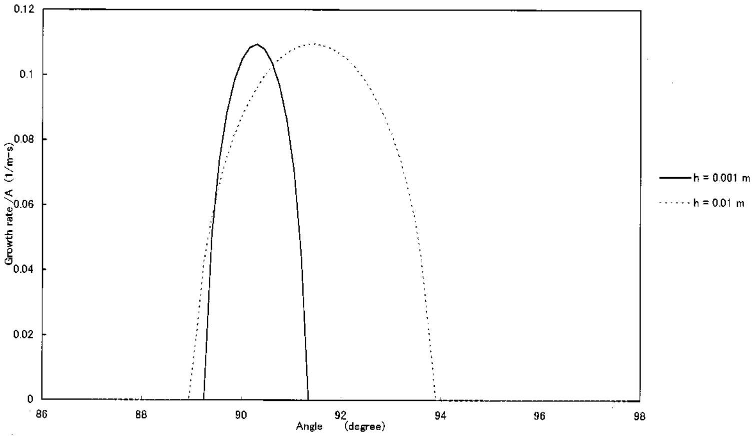

Figure 2. Growth rate of internal waves for different depths of the fluidized layer ($h = 0{\cdot}001, 0{\cdot}01$ m). Water depth $H = 4$ m, wave period $T = 10$ s, and density stratification $\gamma = 0{\cdot}9$.

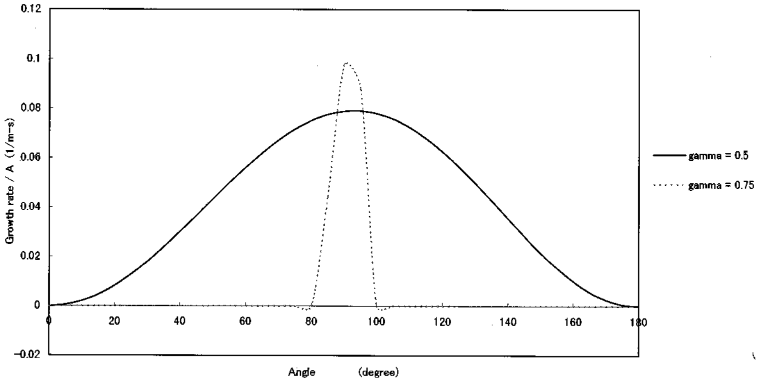

Figure 3. Range of instability for oblique internal waves for different density stratifications ($\gamma = 0{\cdot}5, 0{\cdot}75$). Water depth $H = 4$ m, wave period $T = 10$ s, and the fluidized layer depth $h = 1$ cm.

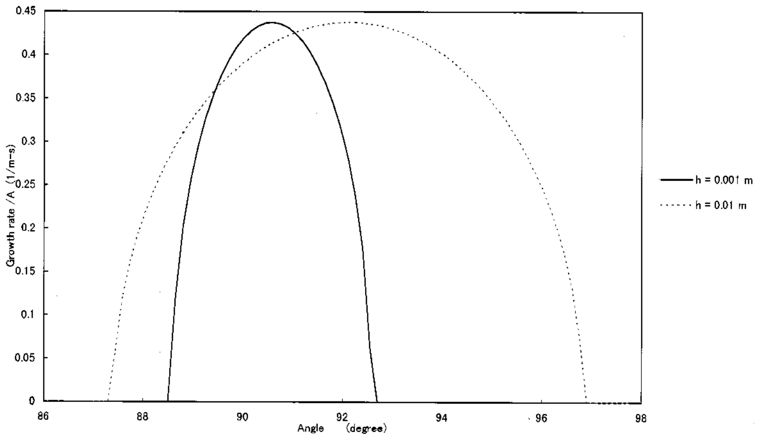

Figure 4. Same as Figure 2, but for a water depth $H = 1$ m.

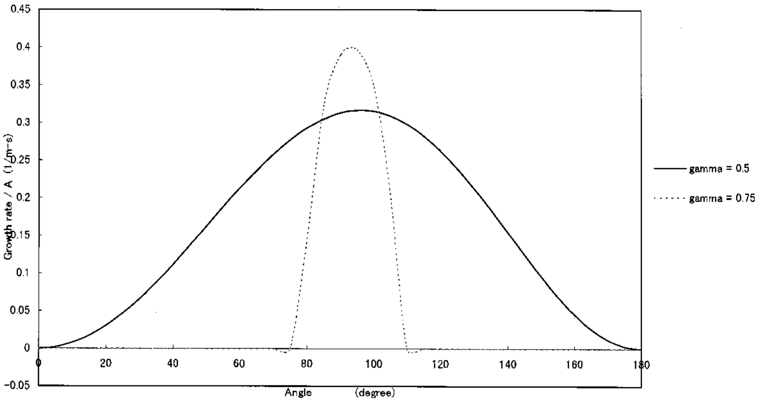

Figure 5. Same as Figure 3, but for a water depth $H = 1$ m.

Next, we turn to the general oblique case. It is easy to see that now $|\lambda_i|$ would replace λ_{ix} in (20). Nevertheless, depending on the angles between the internal modes and the surface mode, the corresponding ratios of k/λ_{ix} are *not* necessarily small in this case. For instance, if the ith internal wave mode is assumed perpendicular to the surface mode, the ratio k/λ_{ix} would become infinite. Note that at such a limit, the growth rate α will be positive and finite (*i.e.* real exponential growth of the internal-wave perturbations). Clearly, also, such an instability should exist within a window around this limit, *i.e.* when the internal waves are almost, but not exactly, perpendicular to the surface wave. Figure 2 gives some indication of the width of this instability window for selected numerical values of the physical parameters.

In Figure 2, the scaled growth rate $\alpha/|A|$ is shown for the case of a water depth $H = 4$ m, wave period $T = 10$ s, density ratio $\gamma = \rho/\rho' = 0{\cdot}9$, and two selected values of the depth h of the fluidized sediment layer: $h = 1$ cm, and $h = 1$ mm. Notice that for the instability to take place, the range of the angle of inclination θ_1 for the internal wave (λ_1, σ_1) is indeed very narrow around $\theta_1 = 90°$. The corresponding angle range for the other internal wave is similarly very narrow around the normal angle too, but is not shown in the figure. It is evident also from Figure 2 that reducing the depth h, from 1 cm to 1 mm, will further reduce the instability range around $\theta_i = 90°$. It is curious, though, that the maximum growth rate for the two h depths is unchanged. The reported inviscid growth rate in the present paper should, however, be viewed as an upper limit for the more realistic viscous behavior in the fluidized sediment layer. We note here, however, that we performed a very preliminary analysis employing a viscoelastic constitutive model for the fluidized slurry, and there were indications that a *stronger-than-inviscid* growth rate may result! Detailed analysis on the effects of non-inviscid constitutive models for the sediment slurry is clearly needed in future studies.

Figure 3 shows an interesting effect of stratification on the range of instability. We note first that, within the context of deeper-water oceanography, even a value of $\gamma = \rho/\rho' = 0{\cdot}9$, as in Figure 2, may be considered too excessive. Indeed, if we restrict the agents for density variations to just salinity and temperature, this γ value appears unrealistically excessive. However, the interest here is on sediment fluidization-induced stratification near the seafloor. In this sense, $\gamma = 0{\cdot}9$ may be viewed as *weak*. Assuming sediment-grain density of about 2600 kg/m^3, then we see that $\gamma = 0{\cdot}9$ would correspond to a solid concentration in the slurry of only 7% by volume, a small value indeed. Figure 3 shows the results for higher sediment concentrations (or lower γ) in the fluidized layer. Clearly, increasing the sediment load in the slurry appears to enhance the range of instability to cover a wider internal-surface wave inclination angles beyond the normal angle $\theta_i = 90°$. Notice that in the case of $\gamma = 0{\cdot}5$ (high solid concentration of about 60%) practically *all* inclination angles are unstable. Furthermore, Figures 4 and 5 repeat the above results at the shallower water depth of $H = 1\,\mathrm{m}$. As shown in these figures, the growth rate is significantly increased by decreasing the water depth. The expanded range and intensity of the instability for such high-concentration, thin fluidized layers under shallower waters certainly adds to the potential importance of this instability at the seafloor interface. One important application, obviously, is to describe the excitation mechanism of Inman's [5] ephemeral ripples. It is believed that the present theory explains the initial development of these ripples. The further evolution of these ripples, as described in [4], including the important events of sand bursting and pluming from the seafloor, will have to await future studies of these generated subharmonic seafloor waves carried beyond the present initial growth phase.

References

1. M. A. Foda and S.-Y. Tzang, Resonant fluidization of silty soil by water waves. *J. Geophy. Res*. 99(C10) (1994) 20463–20475.
2. M.A. Foda and C.-M. Huang, Generation of ripple-size standing sediment waves on the seafloor by progressive water waves, Paper O21E-13 (abstract only), 1994 AGU Fall Meeting, San Francisco, CA, Supplement to EOS, p. 336.
3. J. F. A. Sleath, *Seabed Mechanics*. New York: Wiley-Intersciences (1984) 335 pp.
4. D. C. Conley and D. L. Inman, Field observations of the fluid-granular boundary layer under near-breaking waves. *J. Geophys. Res*. 97(C6) (1992) 9631–9643.
5. D. L. Inman, Wave generated ripples in nearshore sands, *Tech Memo. 100*, U.S. Army Corps of Eng., Beach Erosion Board (1957) 64pp.
6. D. F. Hill and M. A. Foda, Subharmonic resonance of short internal standing waves by progressive surface waves. *J. Fluid Mech*. 321 (1996) 217–234.
7. D. F. Hill and M. A. Foda, Subharmonic resonance of oblique internal waves by a progressive surface wave. To appear in *Proc. R. Soc. London*, Series A (1998).
8. M. A. Foda and D. F. Hill, Nonlinear energy transfer from semi-diurnal barotropic motion to near-inertial baroclinic motion. Submitted to *J. Phys. Oceanogr.* (1997).
9. C. C. Mei, *The Applied Dynamics of Ocean Surface Waves*. New York: Wiley-Intersciences (1983) 740 pp.